/ . 2

4. International conference on valence fluctuations
Cologne (Germany, FR) 27-30 Aug 1984
CEA-CONF--7392

FR8403043

RADIATION DAMAGE IN SmS, $SmS_{1-x}P_x$ and SmB_6

J. Morillo*, G. Bordier*, C.H. de Novion*, J.P. Sénateur** and J. Jun***

* DTech/SESI, CEN, B.P.6 92260 Fontenay-aux-Roses, France

** CNRS, ER 155, IEPG, BP16, 38402 S[t] Martin d'Hères, France

***Research Center for Hard Materials, Zielna, 37, Varsawa, Poland

ABSTRACT

Large conductivity increases under 21 K electron or neutron irradiations are observed in SmS and $SmS_{1-x}P_x$. It is shown that they are related to Sm defects. A possible mechanism is 4f electron delocalization around radiation defects. In SmB_6, the low temperature resistivity increase desappears under 21 K irradiation. The thermal stability of the defects is also investigated up to room temperature.

RESUME

Nous avons observ´ des augmentations importantes de la conductivité de SmS et $SmS_{1-x}P_x$ sous irradiation électronique ou neutronique à 21 K. Nous montrons qu'elles sont associées à des défauts Sm. Un mécanisme possible est la délocalisation d'un électron 4f autour des défauts d'irradiations. Dans SmB_6, la divergence de ρ à basse température est détruite par irradiation à 21 K. Nous avons également étudié la stabilité thermique des défauts jusqu'à 300 K.

INTRODUCTION

When studying binary compounds with only partial ionic character and high melting temperatures we are always faced with the problem of stoichiometry and thermodynamic structural defects, i.e. the presence of uncontrolled concentrations C of point defects in the range 10^{-2}-10^{-6}. They can influence their physical properties and lead to controversial theoretical interpretations, a typical example being the low temperature properties of SmB_6. So we started in our laboratory a systematic study of the influence of radiation damage on the physical properties of those unstable or mixed valence compounds [1, 2, 3, 4]. Radiation damage is indeed one of the most convenient tools for studying point defects in this concentration range. It allows to introduce known concentrations of point defects (i.e. Frenkel pairs) in one of the sublattices and to make a quantitative study of the physical properties of the material as a function of the defect concentration (or irradiation time). We report here the actual state of our investigations of radiation damage in SmS, $SmS_{1-x}P_x$ ($x < 0.04$) and SmB_6 whose electrical conductivities σ (or resistivities ρ) have been measured during low temperature irradiations and subsequent annealings.

EXPERIMENTAL

The irradiated samples were single crystals from the "Laboratoire des Matériaux ER 155" CNRS in Grenoble for SmS and $SmS_{1-x}P_x$ and from the "Research Center for Hard Materials" in Varsawa for SmB_6.

Fast neutrons irradiations at 21 K were performed on the VINKA device of the "Section d'Etude des Solides Irradiés" (SESI) [5] on the CEN-FAR Triton Nuclear Reactor and electrons irradiations at 21 K and 4 K on the VINKAC device (21 K) [6] and in a special Helium cryostat behind the SESI Van de Graaff accelerator at CEN-FAR. The samples were first cooled from 300 K to the irradiating temperature, irradiated then warmed slowly up to 300 K and finally cooled to 21 K or 4 K. The conductivity σ was measured during the whole experiments.

SmS AND $SmS_{1-x}P_x$.

On figure one we have reported the observed variation of the normalized electrical resistivities ρ of SmS and $SmS_{1-x}P_x$ (x = 1%, 3% and 4%) versus concentration of defects (in atomic concentration as calculated hereafter) : the resistivity of SmS is reduced by a factor 10^6 with a 10^{-4} defect concentration. This effect is less and less pronounced when the P concentration is increased and reverses at 4 % P concentration.

Taking into account the n semiconductor character of SmS, this resistivity decrease is related to an increase of the free electron concentration with radiation defects : the concerned defects have a donor character. The most simple explanation is to attribute this effect to 4f electron delocalizations of the Sm interstitials induced by the irradiation, which change their valence from 2+ to 3+ in order to accomodate the smallest volume of the interstitial tetrahedral position. Moreover this explanation is consistent with the observed $SmS_{1-x}P_x$ results.

It must be noted that the Sm vacancy associated to each Sm interstitial induced by the irradiation can also favour $Sm^{2+} \rightarrow Sm^{3+}$ transitions as in LnB_6 [7].

We have assumed that Sm atoms are displaced permanently at 21 K, whereas S atoms are not. This has been confirmed by electron irradiations of SmS at 21 K at various electron energies which allows to measure the cross sections for the displacement of the atoms of each sublattice (figure 2) and hence to determine the threshold energies for the displacement and to calculate the number of defects for any irradiation as we have done for figure 1 irradiations [2, 3].

On figure 3 we have reported the observed variations of the conductivity versus temperature of a SmS sample after an electron irradiation : the defects recombine in at least three temperature stages below room temperature. Similar results have been obtained for neutron irradiations of SmS and $SmS_{1-x}P_x$.

SmB_6.

In order to study the role of the defects and impurities in the low temperature divergence of the resistivity ρ of homogeneous intermediate valence (HIV) SmB_6 we have irradiated it at 21 K with neutrons (high irradiation dose) and at 4 K with electrons (low irradiation dose).

Neutron irradiation

The results of this irradiation are presented on figure 4. The observed conductivity increase in the region

10^{-3} - 10^{-1} defect concentration [8] (fig. 4-a), as well as the quasi-temperature independant $\rho(T)$ curve after irradiation (fig. 4-b) indicates clearly that defects destroy the low temperature ρ divergence in HIV SmB_6 giving good support to the theoretical models for which this divergence is an intrinsic effect like the 4f-5f hybridization gap model.

It can be seen also from figure 4-b, that at high temperature SmB_6 behaves like a metal (ρ has increased with the defect concentration at 300 K) and that most of the introduced defects have not recovered at room temperature.

Electron irradiation

This irradiation was performed at 4.2 K up to a dose of 3 10^{-2} C/cm^2 (i.e. about 10^{-4} defect concentration) [9]. The resistivity was found to decrease linearly with the dose ($\Delta\rho/\rho$ = -20 % at the end of the irradiation). The sample was isochronally recovered up to 300 K and the residual resistivity at 4 K after each recovery step was recorded (fig. 5-a) as well as the $\rho(T)$ curve for T less than 50 K in the semiconducting region (fig. 5-b).

As can be seen from fig. 5-b when the concentration of defects increases both the apparent activation energy for the conduction in the normal semiconducting region (1000/T < 120) and the low temperature saturation limit resistivity are decreased.

As for the neutron irradiation the defects are found to reduce the low temperature divergence of ρ. However it appears that contrary to the neutron case, most of the defects have recovered at room temperature (compare fig. 4-b and 5-a). This can be explained if we remember that the defects produced in an electron irradiation are isolated defects that can easily recombine compared to the complex defects induced by a neutron irradiation. Moreover the high defect concentration reached in the neutron irradiation favours clustering of defects.

CONCLUSION.

In the frame of such a short paper it was not possible to present and discuss all our irradiation results. We have just tried to point out the most interesting ones and send you to the quoted references for a more complete description of our irradiation work on this class of compounds.

REFERENCES

(1) J. MORILLO, C.H. de NOVION and J.P. SENATEUR, J. Physique Colloq. 40, C5-348 (1979).

(2) J. MORILLO, Thesis, Orsay (1981), CEA-R-5221 (1983).

(3) D. LESUEUR, J. MORILLO, H. MUTKA, A. AUDOUARD and J.C. JOUSSET, Rad. Eff. 77, 125 (1983).

(4) J. MORILLO, C.H. de NOVION and J. JUN, Solid State Comm. 48, 315 (1983).

(5) R.R. CONTE and J. DURAL, Revue Phys. Appl. 2, 1 (1967).

(6) J. DURAL, These d'Université, Poitiers, (1980), CEA-R-5091 (1981).

(7) T. KASUYA, J. de Phys. 10, C4, 261 (1976).

(8) The concentration scale is different here from the one in ref. [2] and [4], since here it has been corrected from the contribution of the B(n,α) reaction of ^{10}B with thermal neutrons to the total defect production which was not taken into account in ref. [2] and [4].

(9) The defect concentration is an approximated one calculated with a supposed threshold energy of 25 eV. Since the threshold energy has not been measured yet in SmB_6, this defects can be of Sm type or B type or both. This is also the case for the neutron irradiation.

FIGURE CAPTIONS

Figure 1 : Neutron irradiation of SmS and $SmS_{1-x}P_x$ (x = 1,3 and 4 %) :

- a - Log (ρ/ρ_0) versus Sm defect concentration C. $\rho_0 = \rho_{21K}$ before irradiation.

- b - Same curve as in fig. 1-a for $SmS_{0.96}P_{0.04}$ in a ρ(C) scale.

Figure 2 : Determination of the threshold energy for the displacement E_d^{Sm} in SmS (all curves normalized to E_e = 1.56 MeV) :

- • - experimental points of the rate of increase of the conductivity of SmS under $\bar{e}$ irradiation versus $\bar{e}$ energy E_e.

- — - Calculated cross section for the displacement of Sm with E_d^{Sm} = 20 eV.

Figure 3 : Recovery of defects in SmS after electron irradiation at 21 K. (1) ρ(T) before irradiation. (2) ρ(T) after irradiation. (3) ρ(T) after recovery at 300 K.

- a - in a log ρ vs. 1000/T scale.

- b - in a ρ vs.T scale. The arrows indicate the recovery steps.

Figure 4 : Neutron irradiation of SmB_6 at 21 K :

- a - Log (σ) versus Log C

- b - Lop ρ versus 1000/T : (1) before irradiation. (2) after irradiation and recovery - * ρ(21 K) after irradiation.

Figure 5 : Electron irradiation of SmB_6 at 4 K :

- a - isochronal annealing curve of the resistivity : $\rho(T)$.

T = recovery temperature - all measurements at 4 K.

- b - Log (ρ) vs. 1000/T curves after irradiation and annealing at various temperatures.

figure 1

(a)

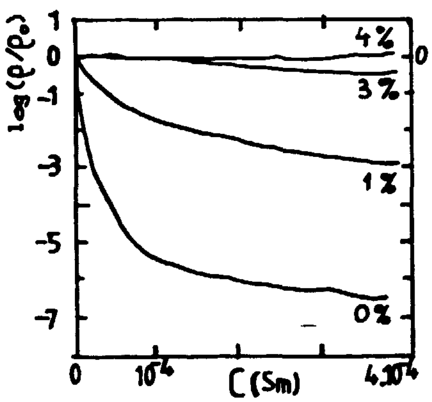
log(ρ/ρ₀)
1
0
-1
-3
-5
-7
4%
3%
1%
0%
0
0
10⁻⁴
C(Sm)
4.10⁻⁴

(b)

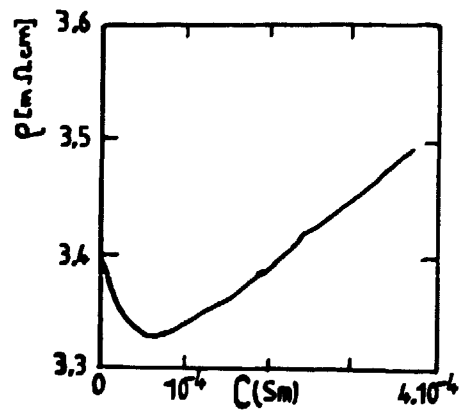
ρ[mΩcm]
3,6
3,5
3,4
3,3
0
10⁻⁴
C(Sm)
4.10⁻⁴

figure 2

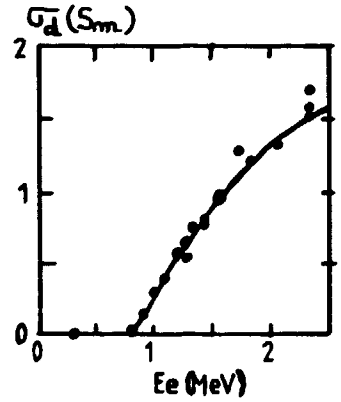

figure 3

(a)

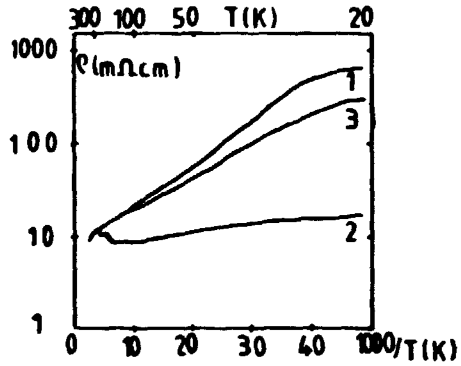
300 100 50 T(K) 20
1000
ρ(mΩcm)
1
3
100
10
2
1
0 10 20 30 40 1000/T(K)

(b)

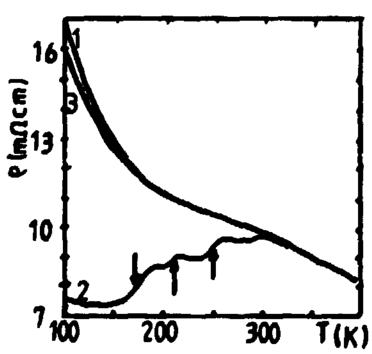
16
1
3
13
ρ(mΩcm)
10
2
7
100 200 300 T(K)

figures 4

(a)

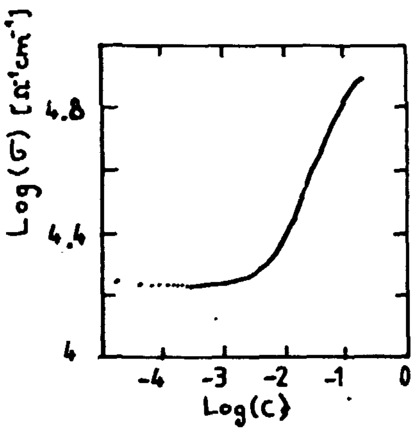

Log(σ) [Ω⁻¹cm⁻¹]
4.8
4.4
4
-4
-3
-2
-1
0
Log(c)

(b)

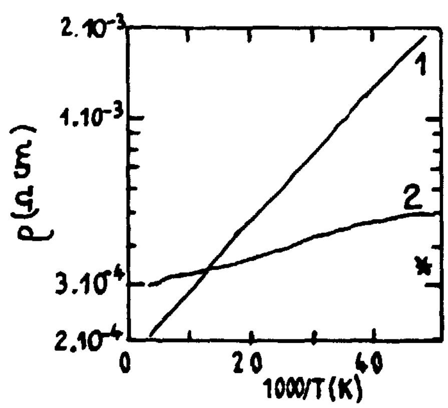

ρ(Ω cm)
2.10⁻³
1.10⁻³
3.10⁻⁴
2.10⁻⁴
1
2
*
0
20
40
1000/T(K)

(a)

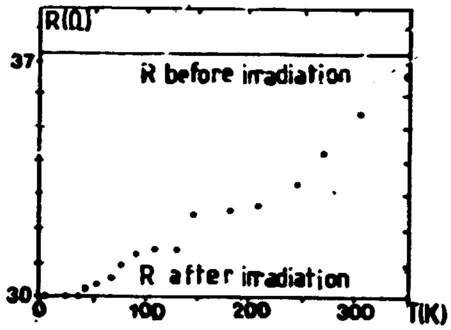

R(Ω)
37
R before irradiation
R after irradiation
30
0
100
200
300
T(K)

(b)

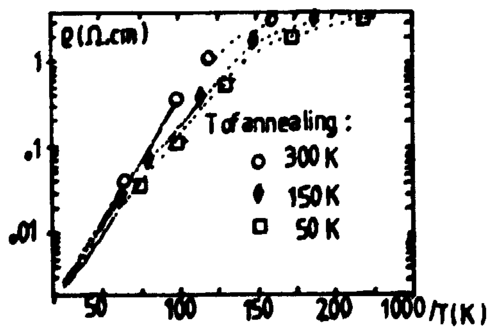

ρ(Ω.cm)
1
.1
.01
T of annealing :
300 K
150 K
50 K
50
100
150
200
1000/T(K)